

Biocide-Free Antifouling on Insulating Surface by Wave-Driven Triboelectrification-Induced Potential Oscillation

Xue Jiao Zhao, Jing Jing Tian, Shuang Yang Kuang, Han Ouyang, Ling Yan, Zhong Lin Wang,* Zhou Li,* and Guang Zhu*

A biocide-free antifouling method on wetted insulating surfaces, enabled by the oscillation of electric potential generated by an integrated triboelectric wave harvester (I-TEWH) is reported. Distinct from previous studies that reported antifouling on conducting surfaces by applying an additional power source, this method achieves antifouling on insulating surfaces with zero-power consumption. The electric potential in the vicinity of a protected surface oscillates in large amplitude as a result of periodically accumulated free electrons on an underlying electrode. The dynamic flow of the free electrons is driven by the I-TEWH that converts ambient wave energy by solid-liquid interface triboelectrification. As a consequence, the oscillating electric potential disturbs the inherent charge distribution on microbes due to electrostatic induction, preventing their initial adhesion onto the protected surface and thus prohibiting the subsequent formation of macroorganisms. Significant anti-adhesion efficiencies of as high as 99.3%, 99.1%, and 96.0% are achieved for negative-gram bacteria (*Escherichia coli*), positive-gram bacteria (*Staphylococcus aureus*), and diatoms (bacillariophyceze), respectively, on a smooth surface. The antifouling efficiency on a roughened surface with micro/nanostructures can be further enhanced by another 75%. This approach can be potentially utilized in coastal constructions, offshore facilities, and vessels that are either moving or stationary in port.

1. Introduction

Biofouling, as its name implies, is the attachment of bacteria and subsequent formation of biofilm and other plants or

Dr. X. J. Zhao, Dr. J. J. Tian, Dr. S. Y. Kuang,
Dr. L. Yan, Prof. Z. L. Wang, Prof. Z. Li, Prof. G. Zhu
Beijing Institute of Nanoenergy and Nanosystems
Chinese Academy of Sciences
National Center for Nanoscience and Technology (NCNST)
Beijing 100083, P. R. China
E-mail: zlwang@binn.cas.cn; lizhou@binn.cas.cn;
zhuguang@binn.cas.cn

Dr. H. Ouyang
Key Laboratory for Biomechanics and Mechanobiology
of Ministry of Education School of Biological Science
and Medical Engineering
Beihang University
Beijing 100191, P. R. China

Prof. Z. L. Wang
School of Materials Science and Engineering
Georgia Institute of Technology
Atlanta, GA 30332, USA

DOI: 10.1002/admi.201600187



animals on wetted surfaces.^[1,2] It poses huge problems to a wide variety of industries wherever water is present, including paper making, food processing, underwater facilities, and desalination plants. Specifically, it is one of the most challenging issues in marine industry, causing impacts to shipping, coastal constructions, oil pipelines, and underwater sensors.^[3-5] For example, the accumulation of biofouling on marine vessels significantly raises the fuel consumption by 40% or \$60 billion per year around the globe.^[3] Therefore, antifouling research has gigantic environmental and economic significance.

Currently, the most widely employed antifouling means is to repel or kill organisms using coatings with biocides, typically tributyltin moiety.^[6] It is toxic not only to targeted microorganisms but also to other larger aquatic species in the vicinity without selection, causing environmental and ecological damage.^[7] In this regard, extensive research efforts have been conducted to develop non-toxic antifouling strategies, including choosing slippery materials,^[8] sacrificing surface materials based on layer-by-layer resolving,^[9,10] creating hydrophilic coatings,^[11] and developing nanoscale surface topologies based on biomimicry.^[12,13] However, these methods have issues such as limited effectiveness to certain species,^[13,14] instability as affected by environment, high cost, and limited duration.^[1,14-16] Particularly, the methods that impose surface potential on an electrically conducting surface to prevent biofouling have been previously reported.^[17,18] This type of antifouling method imposes a loop current through two conducting surfaces between which water with microorganisms flows through. This current-enabled method not only requires an additional power supply but also has the risk of electrochemical corrosion as the conducting surfaces are exposed in the water.

Here, we report a biocide-free antifouling method on insulating surfaces, which is enabled by the oscillation of electric potential generated by an integrated triboelectric wave harvester (I-TEWH) without additional power supplies. The use of electrostatic induction as a result of varying electric potential for antifouling purpose is proposed for the first time. Based on the triboelectrification at the solid-liquid interface, the I-TEWH converts the dynamic mechanical energy of the water wave into electricity.^[19,20] It periodically pumps excessive free electrons

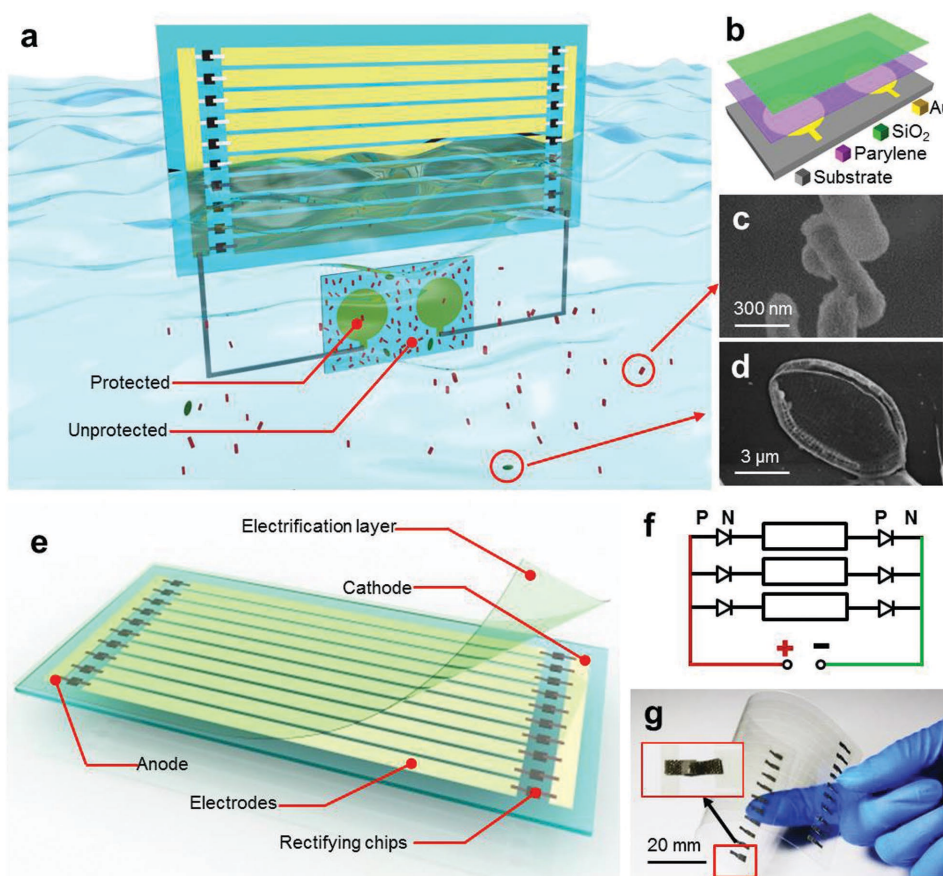


Figure 1. Setup of the self-powered anti-adhesion system and structure of its constituent parts. a) Schematic illustration of the anti-adhesion setup. b) Structure of the underwater component. c,d) SEM images of the *E. coli* and *Nitzschia* Sp. e) Schematic illustration showing the structural design of a thin-film I-TEWH. f) Equivalent circuit diagram of the I-TEWH. g) Photograph showing an as-fabricated flexible I-TEWH, inset: an enlarged view of a p–n junction that regulates the electron flow direction.

onto a conducting layer underneath a protected surface. Then the electric potential in the vicinity of the protected surface is periodically altered. This process in turn disturbs the inherent charge distribution on microbes due to electrostatic induction, preventing the forming of a biofilm and thus subsequent adhesion of macroorganisms.^[18] Our antifouling method is equivalently effective against a variety of organisms and species, including gram-negative and gram-positive bacteria as well as diatoms. Significant anti-adhesion efficiencies of as high as 99.3%, 99.1%, and 96.0% are achieved for *Escherichia coli* (*E. coli*), *Staphylococcus aureus* (*S. aureus*), and bacillariophyceze (*Nitzschia* Sp.), respectively, on a smooth surface. The antifouling efficiency on a roughened surface with micro/nanostructures can be further enhanced by another 75%. More importantly, the oscillation of the electric potential does not rely on an extra power source. Instead, it is driven by I-TEWH that converts ambient wave energy by solid–liquid interface charging without power consumption. Because the I-TEWH is made of thin-film polymeric materials that are cost-effective, it has the promise of being scaled up in area. This unique self-powered feature not only results in superior antifouling efficiencies compared to that by either dc or ac power supplies, but also provides continuous protection around the clock because of the nonstop ambient wave energy. In general, this approach

is suitable to be applied in coastal constructions, offshore facilities, and vessels that are either moving or stationary in port.

2. Results and Discussion

The anti-adhesion setup is presented in **Figure 1a**, which consists of an underwater part and a floating part. The underwater component that needs protection can be split into individual layers, as shown in **Figure 1b**. A substrate is partially covered by two circle-shaped gold electrodes, which are referred to as anti-adhesion electrodes in the following discussions. The sections with and without the anti-adhesion electrodes are denoted as protected and unprotected areas (**Figure 1a**), respectively. Then a layer of parylene is subsequently deposited for waterproofing. The outmost layer surface is made of silicon dioxide, which is purposely selected only for accelerating the adhesion of microorganisms in our experiments due to its hydrophilicity. Biofouling species of bacteria (*E. coli*) and diatoms (*Nitzschia* Sp.) cultured in the ambient water body are shown by scanning electron microscope (SEM) images in **Figure 1c,d**, respectively. It is normally these two types of microorganisms that form the initial biofilm on the surface and thus act as the prerequisite for subsequent adhesion of macroorganisms.^[1,2] The other component that is half-submerged in the water is an I-TEWH. As illustrated in **Figure 1e**,

the I-TEWH has a 2D structure.^[19,20] An array of strip-shaped electrodes is fabricated on a thin-film flexible polyethylene glycol terephthalate (PET) substrate. Each end of the electrodes is connected to a rectifying chip of p–n junction (Figure 1e). For two chips at opposite sides of a single electrode, they are series connected with the polarities aligned in the same direction, as shown by the equivalent circuit diagram in Figure 1f. A pair of the chips on the opposite sides of an electrode serves as “gates” that regulate the flow of induced electrons from the cathode to the anode.^[21] An electrode along with the two rectifying chips is essentially a basic electricity-generation unit. Parallel connected, all of the units share a joint cathode and a joint anode (Figure 1e). The outmost layer is made of polytetrafluoroethylene (PTFE), which serves as both an electrification layer and a waterproofing membrane. The photograph of a fabricated I-TEWH is shown in Figure 1g. With the use of ITO and the flexible thin-film material, it has great transparency and flexibility. The detailed fabrication process is presented in the Experimental Section.

For real operation, one anti-adhesion electrode is connected to the anode while the other is connected to the cathode, as shown in Figure 1a. Ambient wave is generated by periodic agitation of the water container. The interaction between the water and the electrification layer creates negative triboelectric charges on the solid surface.^[22] As the water submerges the thin-film I-TEWH in a repeated way, alternating triboelectric potential tends to induce free electrons to flow in an external circuit. Due to the use of the series connected p–n junctions that regulate the flow of electrons in a single direction, positive induced charges always tend to transport from the anode to the cathode. However, in our case, open-circuit condition applies without charge flow between the anode and the cathode. As a result, excessive induced charges periodically accumulate on the anti-adhesion electrodes. Positive charges appear on the anode side while negative ones exist on the cathode side. This statement is well supported by the measured electric potentials on the anti-adhesion electrodes by an electrometer (Keithley 6514). Figure 2a exhibits

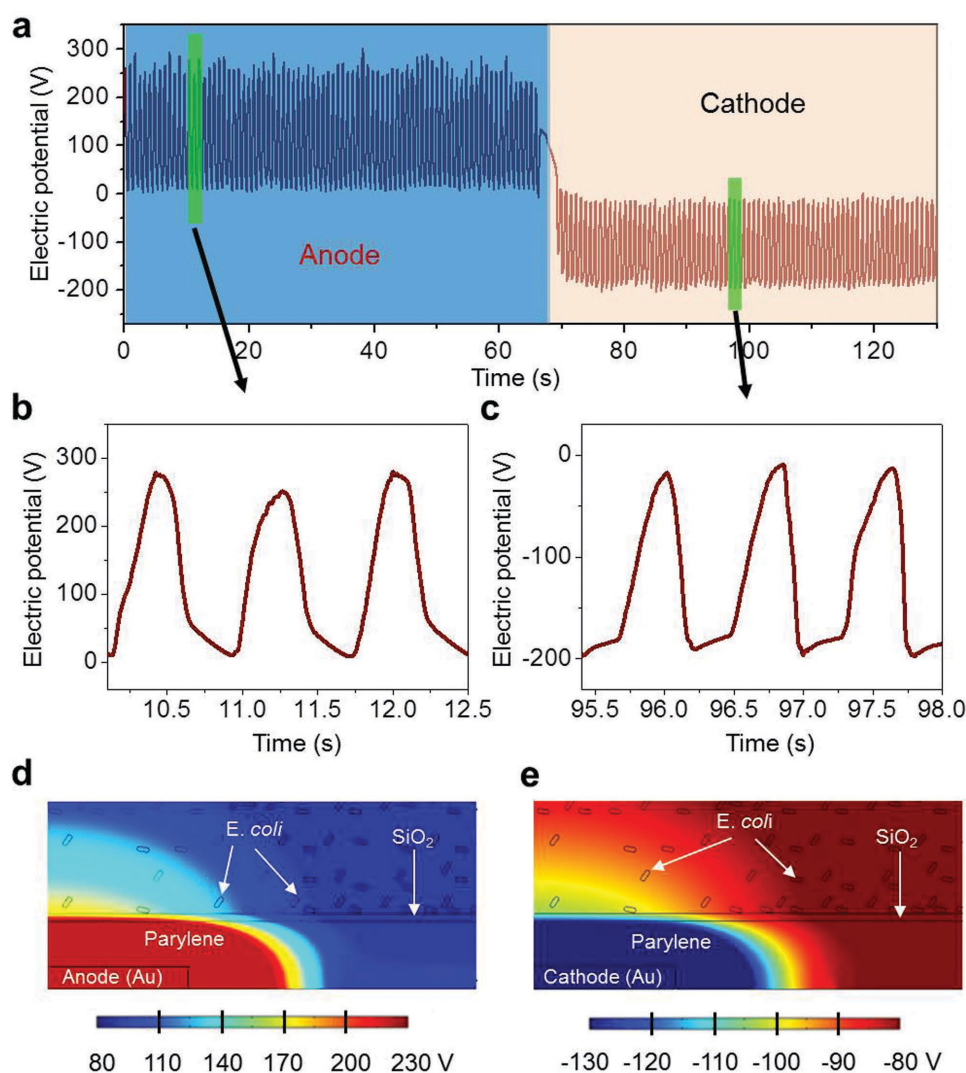


Figure 2. Wave-driven oscillation of electric potential. a) Electric potential measured at the anode and cathode sides of the I-TEWH at a wave frequency of 1.2 Hz. b,c) Enlarged views that show the oscillating behavior of the electric potential at the anode and cathode sides. d,e) Electric potential distributions in the vicinity of the protected and unprotected surfaces via COMSOL simulation.

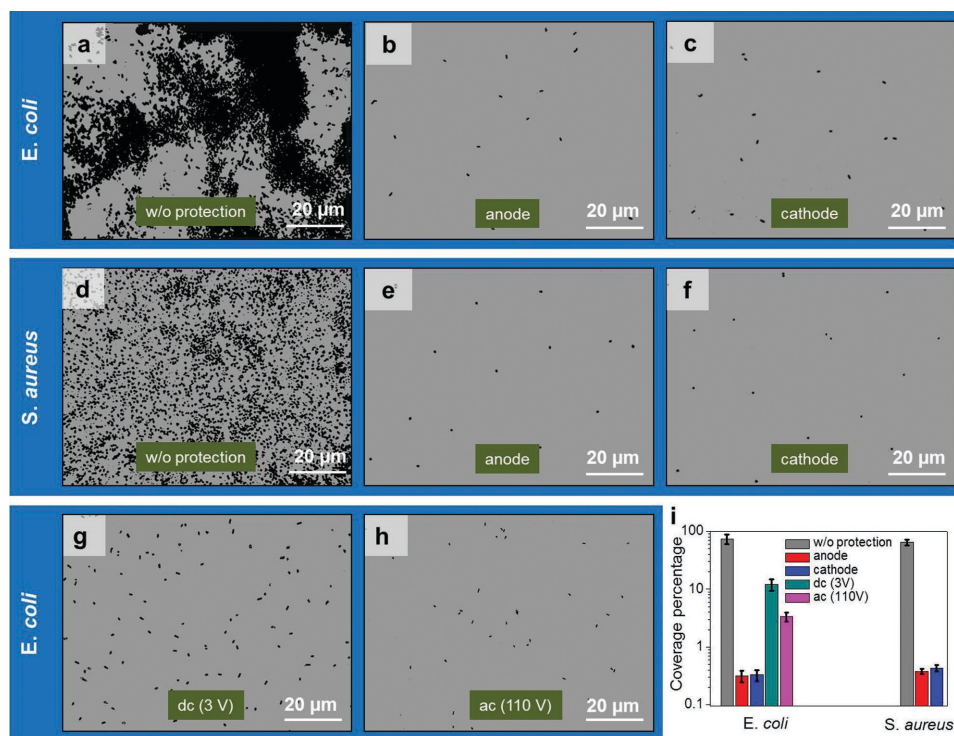


Figure 3. Bacterial attachment results with and without the anti-adhesion protection. Microscopy images showing the anti-adhesion results against a–c) *E. coli* and d–f) *S. aureus*. g,h) Microscopy images showing the anti-adhesion results when powered by an externally supplied dc and ac power source of 3 V. i) Statistical data of area coverage percentages; the y-axis is log-scaled.

the variation of electric potential on the anti-adhesion electrodes as the water interacts with the I-TEWH. At the anode side, the electric potential oscillates in the positive direction, indicating the accumulation of positive induced charges. The peak-to-peak value of the oscillation reaches as high as 200–300 V, as exhibited by the magnified view in Figure 2b. The amplitude fluctuation is attributed to the unstable wave energy. At the cathode side, the polarity of the oscillation is reversed (Figure 2c), which confirms the periodic presence of negative induced charges on the corresponding anti-adhesion electrode. Consequently, an electric potential gradient is created in the vicinity of the protected surface other than the unprotected surface without the underlying anti-adhesion electrodes, which is illustrated by the COMSOL simulation results in Figure 2d,e. In response to the oscillation of the electric potential, an alternating electric field is then produced in the water although it is likely to be rapidly screened because of the water conductivity. It needs to be noted that the electric potential variation is related to the amplitude and the frequency of wave. Higher wave amplitude can result in more induced charges and consequently larger electric potential variation. As for the wave frequency, it can cause faster oscillation of the electric potential. It is reported in literature that most of the microorganisms (e.g., bacteria) are charged entities.^[17,18,23] Electrostatic interaction plays an important role in their adhesion to a wetted surface in the initial stage of biofouling.^[1,2] The alternating electric field can disrupt the surface charge distribution of the microorganisms that are in close proximity to the protected surface.^[18] Consequently, the adhesion by the electrostatic interaction can be substantially inhibited. In this work, we

employed two types of bacteria, i.e., *E. coli* and *S. aureus*, which belong to gram-negative and gram-positive species, respectively. After being submerged in the culture solution with a high concentration of *E. coli* for 24 h, the unprotected surface is adhered by the bacteria that cover 75% of the exposed area. As clearly shown in Figure 3a, severe agglomeration occurs, indicating the formation of bacterial colonies with multi-layered adhesion. In sharp contrast, very little adhesion is observed on the protected surfaces at both the anode (Figure 3b) and the cathode side (Figure 3c).^[13] The coverage percentage (i.e., the percentage of the surface area covered by microbes) drastically reduces to 0.30% and 0.35%, respectively. Here, the anti-adhesion efficiency is defined in the following equation

$$\eta = \frac{S_{w/o} - S_w}{S_{w/o}} \quad (1)$$

where S_w and $S_{w/o}$ are the coverage percentage of the surfaces with and without the protection, respectively. Therefore, the results in Figure 3a,b represent anti-adhesion efficiencies of 99.6% and 99.3%, respectively. This result is significantly superior to recently reported results in laboratories by other methods. For example, Chung et al. achieved an anti-adhesion efficiency of 87% using a bio-inspired surface.^[10,13] It is found that obvious anti-adhesion effect is equivalently achieved at both the anode and the cathode side, which proves the correctness of our proposed mechanism since the alternating electric field is generated at both sides. Due to the similar reasoning, our approach is also effective to *S. aureus*, a type of gram-positive bacterium

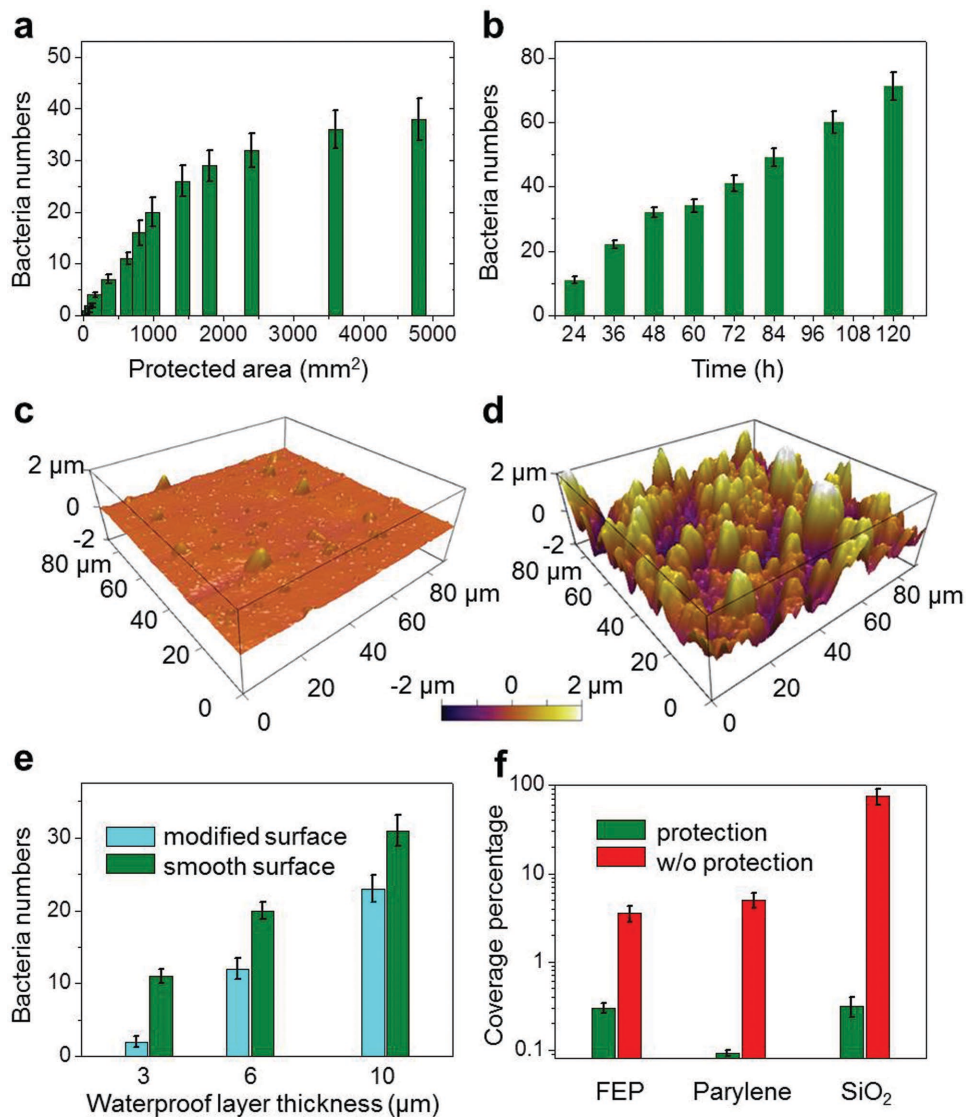


Figure 4. Factors that influence the anti-adhesion efficiencies against *E. coli*. The attached bacteria numbers in an area of $100\ \mu\text{m} \times 75\ \mu\text{m}$ as a) the total protected area and b) the biofouling time increases. c,d) Surface morphology images via AFM of the protected before and after the roughening treatment. e) The number of the attached *E. coli* in an area of $100\ \mu\text{m} \times 75\ \mu\text{m}$ with and without the surface treatment as the thickness of the parylene waterproof layer increases. f) The number of the attached *E. coli* in an area of $100\ \mu\text{m} \times 75\ \mu\text{m}$ with and without the protection when different surface materials are used.

which has much thicker cell walls.^[24,25] Drastic contrast with an anti-adhesion efficiency of over 99.4% (anode, Figure 3e) and 99.1% (cathode, Figure 3f) can be obtained. The surprisingly effective results are likely to be attributed to the high alternating electric field resulting from the large amplitude of the varying electric potential shown in Figure 2. If the I-TEWH is replaced by an external dc (3 V) and ac (110 V) power sources, the coverage percentage becomes 12.1% and 3.4%, giving the anti-adhesion efficiencies of 83.9% and 95.5%, respectively, which explicitly proves the superiority of our wave-driven method. The statistical data are diagrammed in Figure 3i, which clearly exhibits the significant suppression of bacteria adhesion.

We further investigated a series of factors that can influence the anti-adhesion efficiency. First, as the area of the anti-adhesion electrodes increases, the number of settled bacteria also increases (Figure 4a). This is because of the reduced

charge density on the anti-adhesion electrodes, which in turn leads to weakened electric potential variation. It is worth noting that effective anti-adhesion can still be obtained without the formation of bacterial colonies (Figure S1a–d, Supporting Information) even when the entire protected area reaches up to $4800\ \text{mm}^2$ that equals to that of the I-TEWH. Second, submerging time is another important factor. The attached bacteria number on the protected surface is in an approximately linear relation with the submerging time, as shown in Figure 4b. The increase rate is much lower than that on the unprotected surface. Similar increase rate is also observed in previous studies.^[16,26] After 120 h, still no agglomerated colonies could be observed (Figure S1e,f, Supporting Information). Third, the morphology of the protected surface also played an important role. Here, we compared the results between two types of surface roughness, i.e., a smooth surface shown in

Figure 4c and a roughened one by sandpaper polishing shown in Figure 4d. It is observed that the roughing treatment contributes to substantially reduced bacteria number, as revealed in Figure 4e. This anti-adhesion enhancement can be attributed to two likely reasons. The first is the promoted hydrophobicity as a result of the surface roughness.^[15] As shown in Figure S2a (Supporting Information), the attachment of *E. coli* bacteria on roughened surface even without connection to the I-TEWH is greatly reduced as compared to the results on a smooth surface in Figure 3a. The second reason is the enhanced electric field at local sites due to the roughened surface, which makes the variation of the electric potential more drastic (Figure S2b, Supporting Information).^[27] In this regard, the above results indicate that the I-TEWH-enabled method has the promise of being used in conjunction with other means such as surface modification in order to achieve substantially better protection results. Besides, the thicknesses of the electrification layer can also influence the anti-adhesion efficiency in a considerable way. As the thickness decreases, the electric field at the vicinity

of the protected surface becomes magnified. Consequently, better protection results can be obtained (Figure 4e). In addition, the material of the exposed surface is another governing factor. Though we used hydrophilic SiO₂ to facilitate adhesion experiments, it is hydrophobic materials that can further suppress the bacterial adhesion,^[28] which is explicitly exhibited in Figure 4f. It is noticed that parylene results in the minimum number of attached bacteria since it has the smallest thickness (6 μm) compared to that of the fluorinated ethylene propylene (FEP) layer (30 μm). Therefore, our electric-potential-driven approach can be used along with superhydrophobic surfaces in real applications to achieve the maximum anti-adhesion results.

It is known that bacteria and diatoms are the two major microorganisms that contribute to the initial forming of the bio-adhesion.^[1,2] Some previously reported non-biocide anti-fouling techniques were selective to certain species.^[1,14–16] In comparison, our approach is proved to have a wide applicability. As shown in Figure 5a,b, our method is also highly effective to *Nitzschia* Sp., a common benthic diatom. After 48 h, the

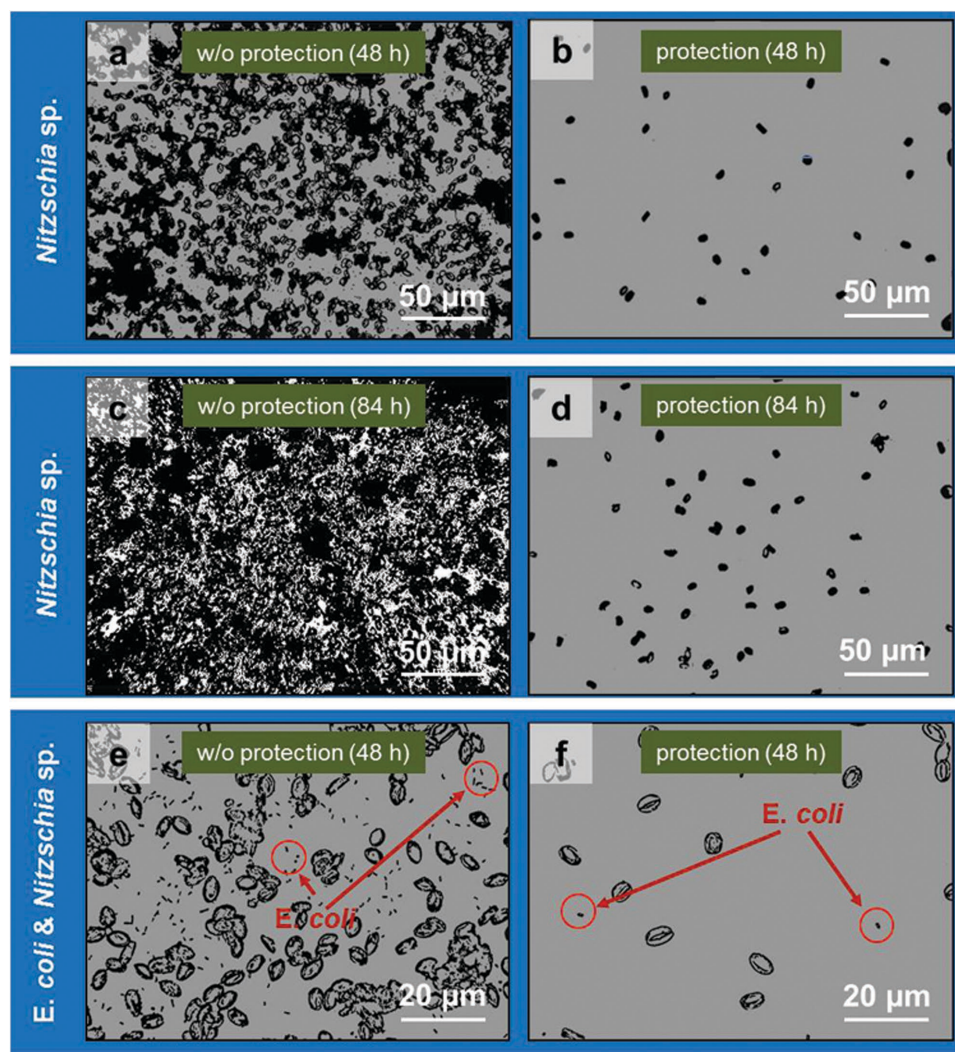


Figure 5. Anti-adhesion results against *Nitzschia* Sp. Anti-adhesion results after a,b) 48 and c,d) 84 h. e,f) Attachment results against the mixture of *E. coli* and *Nitzschia* Sp. after 48 h.

unprotected surface is heavily fouled with 79.6% of coverage, which is otherwise reduced to 3.1% if the protection is applied. As the fouling time increases to 84 h, the anti-adhesion efficiency becomes more obvious (94.6%) In contrast, the number of the adhered diatoms is doubled on unprotected surface which shows the possibility of our method for long-time protection against diatoms. Moreover, Figure 5e,f demonstrates that this anti-adhesion method can simultaneously protect against both *E. coli* and *Nitzschia Sp.* that co-exist after 48 h.

3. Conclusion

In conclusion, we propose an effective and general anti-adhesion measure against microorganisms based on the oscillation of electric potential driven by a thin-film I-TEWH. The oscillating electric potential is able to disturb the charge distribution of microorganisms in the vicinity of the protected surface, which drastically suppresses microbes' adhesion. Our anti-adhesion method not only presents a new strategy against biofouling but also possesses the following prominent features. First, it yields substantially high anti-adhesion efficiency due to the large amplitude of the electric potential variation. Second, it is equivalently effective to a variety of species, including bacteria and diatoms. Third, driven by non-stop ambient wave, it provides perpetual protection without the reliance of external power sources. Fourth, area-scalable protection is achieved, indicating it as a cost-effective and practical technique. Besides, this method is biocide-free, making it environmentally friendly. It has the possibility of being used in conjunction with other strategies such as superhydrophobic materials and micro-patterned surface morphology to maximize the antifouling effectiveness.

4. Experimental Section

Fabrication of the Thin-Film I-TEWH: A PET substrate (100 mm × 60 mm × 150 μm) was prepared by laser cutting. A PET-based mask with hollow windows that define the positions and dimensions of the strip-shaped electrodes (80 mm × 4.8 mm for each, a total of 11 units as an interval of 0.7 mm), the anode (5 mm × 65 mm), and the cathode (5 mm × 65 mm) was also prepared by laser cutting. Through rf-sputtering, an ITO layer (200 nm in thickness) was deposited onto the PET substrate. Chips of p–n junctions were used to connect the strip electrodes to the anode/cathode. The bottom side of the p–n junctions was adhered onto the strip electrodes by conductive copper tapes, while the top side of junctions was connected to either anode or cathode by conductive copper tapes. A PTFE film of 30 μm in thickness with adhesive on one side was used to cover the entire substrate.

Fabrication of Underwater Components: Two circle-shaped Au electrodes were deposited by sputtering on a Kapton substrate that was already cleaned by ultrasonication in acetone and then alcohol for 2 min. The interval between the electrodes was 5 mm. Then an insulating layer of parylene-C was deposited onto the electrodes by PDS2010 (Specialty Coating System). The thickness of the parylene layer was controlled by the deposition time. If another material was added as the outmost layer, it was fabricated by a corresponding technique. For silicon dioxide, a thin film of 1 μm was sequentially deposited by plasma enhanced chemical vapor deposition. For FEP, a layer of 30 μm thick was adhered onto the substrate. In order to enhance the bonding strength between different layers of materials for complete waterproofing, oxygen plasma treatment of 5 min was carried out before the deposition of each layer.

The surface roughening treatment was achieved by sand-polishing the Kapton substrate using fine grit sandpaper (2000 #) before making the anti-adhesion electrodes.

Electrical Output Measurement of the I-TEWH: The wave energy harvester was attached on the side wall of a water tank. Agitation was applied on the opposite side of the tank to generate propagating water waves that repeatedly submerged the I-TEWH. Keithley 6514 electrometer was used to measure the electric potential on the anti-adhesion electrodes. The positive terminal was connected to either the anode or the cathode, while the negative terminal was grounded.

Observation and Counting Methods: The adhesion images were taken by metallurgical microscopy at the 500 and 200 times of magnification for observing bacteria and diatom, respectively. In order to obtain the average numbers of the attached bacteria, an anti-adhesion electrode was divided into segments. 13 areas that uniformly distributed on the protected surface were selected to obtain the statistical numbers of the attached bacteria (Figure S3, Supporting Information).

Culture of Bacteria: Two model bacteria *E. coli* CICC 23657 and *S. aureus* CICC 10384, which represent Gram-negative and Gram-positive species, were selected to evaluate the anti-adhesion effect. *E. coli* and *S. aureus* were obtained from the China Center of Industrial Culture Collection (CICC). Freeze-dried bacteria were activated according to the CICC guidelines. Bacteria were grown in Luria–Bertani (LB) broth^[29] containing 0.3% beef extract, 1% peptone, and 0.5% NaCl. Then activated bacteria were inoculated into a 250 mL Erlenmeyer flask and cultivated with shaking (120 rpm) at 37 °C.

The bacteria in logarithmic phase were acquired after shaking at 37 °C for 5 h.^[30,31] After that the underwater component was put into bacteria solution and co-cultured for different time. Then the underwater component was washed with phosphate buffered saline (PBS) three times to remove the bacteria that not adhered. At last, the bacteria were dyed using Gram staining kit to capture the bright field images taken by metallurgical microscopy.

Culture of *Nitzschia Sp.*: *Nitzschia Sp.* is a gift from Algal Biotechnology Laboratory of College of Life Science, Yantai University.^[32] The synthetic seawater was prepared by adding sea salt (32 g L⁻¹) to distilled water. Then F2 medium with added sodium silicate (Table S1, Supporting Information) was prepared for *Nitzschia Sp.* growth. After that, the *Nitzschia Sp.* cells were inoculated in a 250 mL Erlenmeyer flask and maintained at 25 °C under a 12:12 h light:dark cycle (natural light without direct sunlight).^[33]

Nitzschia Sp. cells in logarithmic growth phase were collected by incubated for 5 d after inoculation^[34,35] at above culture condition. After that the underwater components were put into F2 cultured medium and co-cultured with *Nitzschia Sp.* for different time to evaluate the anti-adhesion effect. Then the sample was washed with PBS three times to remove the *Nitzschia Sp.* that not adhered. At last, the cells were counted under optical microscope taken by metallurgical microscopy.

Supporting Information

Supporting Information is available from the Wiley Online Library or from the author.

Acknowledgements

X.J.Z. and J.J.T. contributed equally to this work. The research was supported by the Chinese “thousands talents” program for pioneer researchers and the innovation team, NSFC 31571006, NSFC 51572030, and Beijing Nova Program Z121103002512019. Patents have been filed based on the research presented here.

Received: March 6, 2016

Revised: June 8, 2016

Published online:

- [1] J. A. Callow, M. E. Callow, *Nat. Commun.* **2011**, *2*, 244.
- [2] M. Lejars, A. Margaillan, C. Bressy, *Chem. Rev.* **2012**, *112*, 4347.
- [3] M. P. Schultz, J. A. Bendick, E. R. Holm, W. M. Hertel, *Biofouling* **2010**, *27*, 87.
- [4] C. E. Marcato-Romain, Y. Pechaud, E. Paul, E. Girbal-Neuhausser, V. Dossat-Létisse, *Biofouling* **2012**, *28*, 305.
- [5] N. Wisniewski, M. Reichert, *Colloids Surf., B* **2000**, *18*, 197.
- [6] P. Gibbs, G. Bryan, *J. Mar. Biol. Assoc. UK* **1986**, *66*, 767.
- [7] F. A. Guardiola, A. Cuesta, J. Meseguer, M. A. Esteban, *Int. J. Mol. Sci.* **2012**, *13*, 1541.
- [8] M. Kolar, U. Schmidt, E. Kuismanen, M. S. Salkinoja-Salonen, *J. Bacteriol.* **2002**, *184*, 2473.
- [9] T. H. Duong, J.-F. Briand, A. Margaillan, C. Bressy, *ACS Appl. Mater. Interfaces* **2015**, *7*, 15578.
- [10] M. L. Hawkins, F. Fay, K. Rehel, I. Linossier, M. A. Grunlan, *Biofouling* **2014**, *30*, 247.
- [11] I. Banerjee, R. C. Pangule, R. S. Kane, *Adv. Mater.* **2011**, *23*, 690.
- [12] C. M. Magin, S. P. Cooper, A. B. Brennan, *Mater. Today* **2010**, *13*, 36.
- [13] K. K. Chung, J. F. Schumacher, E. M. Sampson, R. A. Burne, P. J. Antonelli, A. B. Brennan, *Biointerphases* **2007**, *2*, 89.
- [14] P. J. Molino, E. Campbell, R. Wetherbee, *Biofouling* **2009**, *25*, 685.
- [15] M. Lorenzetti, I. Dogša, T. Stošicki, D. Stopar, M. Kalin, S. Kobe, S. Novak, *ACS Appl. Mater. Interfaces* **2015**, *7*, 1644.
- [16] J. M.-Y. Chiu, V. Thiagarajan, J. A. Pechenik, O.-S. Hung, P.-Y. Qian, *Mar. Biol.* **2007**, *151*, 1417.
- [17] S. Shim, S. H. Hong, Y. Tak, J. Yoon, *Biofouling* **2011**, *27*, 217.
- [18] P. v. Zumbusch, W. Kulcke, G. Brunner, *J. Membr. Sci.* **1998**, *142*, 75.
- [19] G. Zhu, Y. Su, P. Bai, J. Chen, Q. Jing, W. Yang, Z. L. Wang, *ACS Nano* **2014**, *8*, 6031.
- [20] X. J. Zhao, G. Zhu, Y. J. Fan, H. Y. Li, Z. L. Wang, *ACS Nano* **2015**, *9*, 7671.
- [21] X. S. Meng, Z. L. Wang, G. Zhu, *Adv. Mater.* **2015**, *28*, 668.
- [22] G. von Heijne, *J. Mol. Biol.* **1986**, *192*, 287.
- [23] K. Yatsuzuka, Y. Mizuno, K. Asano, *J. Electrostat.* **1994**, *32*, 157.
- [24] S. Rodrigues, A. Varandas, *Phys. Chem. Chem. Phys.* **2000**, *2*, 435.
- [25] C. Cummins, H. Harris, *Microbiology* **1956**, *14*, 583.
- [26] A. Reisch, J. Hemmerlé, A. Chassepot, M. Lefort, N. Benkirane-Jessel, E. Candolfi, P. Mésini, V. Letscher-Bru, J.-C. Voegel, P. Schaaf, *Soft Matter* **2010**, *6*, 1503.
- [27] C. Liu, X. Xie, W. Zhao, J. Yao, D. Kong, A. B. Boehm, Y. Cui, *Nano Lett.* **2014**, *14*, 5603.
- [28] A. Cordeiro, M. Nitschke, A. Janke, R. Helbig, F. D'Souza, G. Donnelly, P. Willemsen, C. Werner, *eXPRESS Polym. Lett.* **2009**, *3*, 70.
- [29] E. A. Adelberg, M. Mandel, G. Chen, *Biochem. Biophys. Res. Commun.* **1965**, *18*, 788.
- [30] C. Sekse, J. Bohlin, E. Skjerve, G. E. Vegarud, *Microb. Inf. Exp.* **2012**, *2*, 1.
- [31] H. Fujikawa, A. Kai, S. Morozumi, *Food Microbiol.* **2004**, *21*, 501.
- [32] Q. Su, R. L. Xing, H. Y. Wang, *Adv. Mater. Res.* **2012**, *518*, 549.
- [33] H. V. Dao, V. B. Phan, S. T. Teng, H. Uchida, C. P. Leaw, P. T. Lim, T. Suzuki, K. X. Pham, *Fish. Sci.* **2015**, *81*, 533.
- [34] J. F. C. De Brouwer, L. J. Stal, *J. Phycol.* **2002**, *38*, 464.
- [35] D. J. Smith, G. J. C. Underwood, *J. Phycol.* **2000**, *36*, 321.